

# INTERNATIONAL SOCIETY FOR SOIL MECHANICS AND GEOTECHNICAL ENGINEERING



*This paper was downloaded from the Online Library of the International Society for Soil Mechanics and Geotechnical Engineering (ISSMGE). The library is available here:*

<https://www.issmge.org/publications/online-library>

*This is an open-access database that archives thousands of papers published under the Auspices of the ISSMGE and maintained by the Innovation and Development Committee of ISSMGE.*

*The paper was published in the proceedings of the 10th European Conference on Numerical Methods in Geotechnical Engineering and was edited by Lidija Zdravkovic, Stavroula Kontoe, Aikaterini Tsiampousi and David Taborda. The conference was held from June 26<sup>th</sup> to June 28<sup>th</sup> 2023 at the Imperial College London, United Kingdom.*

*To see the complete list of papers in the proceedings visit the link below:*

<https://issmge.org/files/NUMGE2023-Preface.pdf>

# Effects of fines content in numerical simulation of CPTu in silty sands

S.S. Nagula<sup>1</sup>, H.P. Jostad<sup>1</sup>, Ø. Blaker<sup>1</sup>

<sup>1</sup>Norwegian Geotechnical Institute (NGI), Oslo, Norway

**ABSTRACT:** The Cone Penetration Test (CPTu) does not measure soil properties directly; rather, it measures cone resistance, sleeve friction and pore water pressure, that correlated with laboratory test data, allow estimation of soil properties. These correlations work reasonably well in clean sand; however, they have been observed to provide poor estimation when fines are present. The aim of this work is to improve the estimation of fine contents in silty sands from CPTu measurements. Large-deformation finite element analyses in ABAQUS implicit scheme with the "zipper technique" is used to simulate CPTu. The SANISAND model is used to capture the soil behaviour and account for fines content by altering the critical state line. Coupled consolidation analyses are performed to account for development of pore pressures during cone penetration. The influence of fines and drainage on the tip resistance and developed pore pressure is analysed. Existing field CPTu measurements would be back calculated using laboratory test data, to ascertain the accuracy of the developed framework. The results are analysed in tandem to improve the understanding of effect of fines content on CPTu response.

**Keywords:** Silty Sands; CPTu; FEM; Zipper Technique; Coupled Analysis

## 1 INTRODUCTION

In the offshore industry Gravity Based Foundations (GBF) are shallow foundations that derive their stability from the self-weight of the foundation and resistance offered by the underlying ground. They are considered competitive in nearshore windfarms at shallow water depths (<10 m water depth) or at locations with deeper waters and rocky soils where pile driving may be difficult or when underwater pile driving noise needs to be avoided to protect wildlife (NREL 2022). The feasibility of such a GBF is often highly dependent on the details of the soil stratification in the upper 5 to 10 metres (Kort et al., 2016). One of the key factors that drives the design of GBF is its resistance against sliding. This requires identification of continuous (thin) weak clay or silt layers below the foundation footprint, creating a potential horizontal failure plane below the GBF. Yang (2004) illustrated the effect of non-plastic fines (particles < 0.063 mm) on the undrained shear strength of a sand, showing a tremendous loss of shear strength when the fines content (FC) exceeds 10% to 20%, depending on the relative density ( $D_r$ ) of the specimen and the confinement stress.

The offshore wind industry relies heavily on the cone penetration test (CPTu) for measuring the in-situ soil conditions and characterising large areas with numerous turbine structure locations. Interpretation of CPT data is largely dependent on site-specific or published correlations to determine characteristic design parameters for various soil layers used for design of foundations. In

sands, these correlations work reasonably well when there is limited number of fines particles in the voids (clean sand). However, they provide poor estimation of soil properties when fines are present (e.g., in silty sands). Underestimating the properties of these critical silty soil layers can potentially have an ill-impact on the design of GBF.

Several correlations for estimation of fines content from CPT data have been proposed in recent years (Cetin & Ozan, 2009; Idriss & Boulanger, 2008; Robertson & Wride, 1998). However, Yi (2014) shows that these correlations underpredict fines contents. Application of regression-based correlations can be especially problematic in thinly interlayered soil deposits, where spatial variability of soil behaviour is greater, and measurements may be unreliable. It is common to develop site specific CPT correlations to estimate fines content (Basal et al., 2022) but this approach might not be very suitable for the offshore industry.

In this work we simulate CPTu in a large deformation finite element method (LDFEM) framework using an appropriate constitutive model, the SANISAND model (Dafalias and Manzari, 2004). The objective is two legged, first to study the influence of fines content on CPTu tip resistance measurements and second to check the ability of the framework to replicate CPTu measurements from an offshore wind farm site with presence of silty sand layers.

## 2 NUMERICAL FRAMEWORK AND METHODOLOGY

This section briefly describes the attributes of the numerical framework along with the chosen constitutive model to simulate the silty sand behaviour. The effect of fines content on sand behaviour and its effect on material parameters are also discussed.

### 2.1 Numerical model to simulate CPTu

The numerical simulation of the CPTu requires simulation of large relative displacements between the cone and the soil. The CPTu, hence, was simulated based on the Zipper technique in a Lagrangian axisymmetric model (Cudmani, 2001; Grabe and König, 2004). This method includes a frictionless tube with a diameter of 1 mm along the axis of symmetry of the numerical model over which the cone glided to establish contact between the soil and cone. An axisymmetric model with a radius of 1 m and height of 1 m was created as shown in Figure 1. A cone with a diameter of 16 or 36 mm ( $D_{cone}$ ) was modelled as a rigid body with a separate rigid body imitating the sleeve of the cone, to distinguish the tip resistance from the total resistance. Typically, a CPT cone has a cone angle of  $60^\circ$  and the same was modelled. But the cone tip had to be smoothed to avoid numerical instabilities due to sharp corners made by the  $60^\circ$  angle. The lower edge of the model was completely fixed. In coupled simulations involving pore water and drainage, the top edge of the model was set to maintain hydrostatic pore pressure to act as the drainage. The right edge of the model was fixed laterally. At the beginning of the simulation, the cone was pre-installed at a depth of  $5D_{cone}$ . The in-situ vertical stress on the soil layer was simulated as an external surface load, as shown in Figure 1. This ensured a homogeneous stress state with uniform void ratio ( $e$ ) in the entire soil. The soil was discretized with 6039 CAX4R 4-noded elements with reduced integration. The mesh was refined along the cone trajectory. The contact between the CPT and the soil was modelled according to Coulomb's friction law. Coulomb's friction law with wall friction coefficient  $\mu = \tan(\delta)$  was considered (Chmelnizkij et al., 2017) where  $\delta$  is the angle of interface friction considered as  $0.5 \phi$  where,  $\phi$  is the peak angle of internal friction (Durgunoglu and Mitchell, 1975). Hard contact was assumed in the normal direction. An implicit integration scheme in ABAQUS Standard 6.14 was used.

### 2.2 Simulation phases

Different initial state conditions were simulated in terms of the initial void ratio and vertical stress, and the corresponding tip resistance under each case was calculated. The simulation of CPT was sequenced as per the following steps.

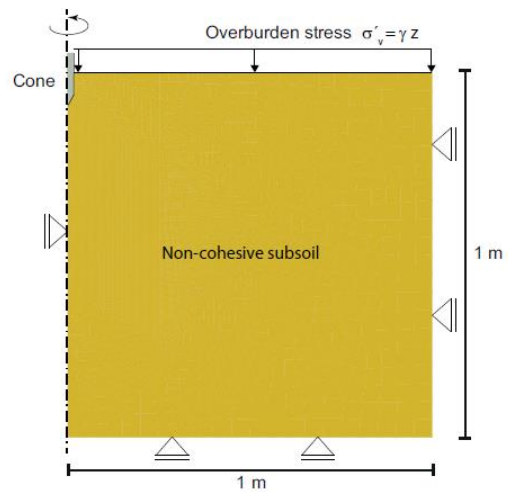


Figure 1. 2D axisymmetric Finite Element Model based on the Zipper technique with a 1 mm rigid tube along centreline to model penetration of CPTu

**Initial Phase:** Activation of model geometries, contact conditions and boundary conditions. The CPT was wished-in-place at a depth of  $5D_{cone}$ .

**Stress State:** The initial stress state in terms of the effective vertical stress and initial void ratio was activated.

**CPT Penetration:** The cone was penetrating the soil at a displacement rate of 20 mm/s until a constant tip resistance was reached.

### 2.3 SANISAND constitutive model

The SANISAND model (Dafalias and Manzari, 2004) belongs to the bounding surface family of models. The model is an elastoplastic model based on the concept of critical state soil mechanics and has been demonstrated to be able to simulate drained and undrained behaviour of sand for a wide range of soil densities and stresses (Jostad et al., 2020). The SANISAND model can be calibrated based on the results of laboratory drained and/or undrained triaxial tests. The detailed calibration procedure is described in Dafalias and Manzari (2004).

#### 2.3.1 Capturing the effect of fines

In addition to void ratio ( $e$ ) and mean effective stress ( $p'$ ), fines content heavily affects the mechanical behaviour of sand-silt mixtures. Yin et al. (2016) indicated that the location of the critical state line (CSL) will be altered depending on varying amount of fines content in the sand-silt mixtures. Wei and Yang (2019) demonstrated that the critical void ratio reduces with fines content to about 30 % of fines and then increases with higher percentages of fines. The SANISAND parameters for clean Toyoura sand and that with 10 % and 20 % fines content were taken after Wei and Yang (2019) as tabulated in Table 1. The presence of fines led to variation in the CSL line as demonstrated in Figure 2 as evaluated as per Equation 1.

$$e_{cr} = e_0 - \lambda \left( \frac{p'}{p_{atm}} \right)^\xi \quad (1)$$

where,  $e_{cr}$  = critical void ratio,  $e_0$  = reference void ratio at  $p = 0$  kPa,  $\lambda$  = slope of CSL line  $p'$  = mean effective stress,  $p_{atm}$  = atmospheric pressure and  $\xi$  = exponent that controls the curvature of the CSL.

It is to be noted that Table 1 also tabulates permeability values for wholeness, but they are not SANISAND input parameters.

Table 1. SANISAND Parameters for Toyoura sand with fines after Wei and Yang (2019)

Parameter	0 %	10 %	20 %
$G_0$ (-)	145	145	145
$\nu$ (-)	0.2	0.2	0.2
$M$ (-)	1.21	1.24	1.29
$c$ (-)	-	-	-
$\lambda_c$ (-)	0.0225	0.0357	0.0388
$e_0$ (-)	0.9427	0.917	0.8657
$\xi$ (-)	0.6	0.6	0.6
$m$ (-)	3.5	3.5	3.5
$h_0$ (-)	33	33	33
$c_h$ (-)	0.9	0.9	0.9
$n^b$ (-)	1.1	1.1	1.1
$A_0$ (-)	0.537	0.537	0.537
$n^d$	3.5	3.5	3.5
$z_{max}$ (-)	5	5	5
$c_z$ (-)	600	600	600
$k$ (m/s)	$1.7 \times 10^{-2}$	$1.7 \times 10^{-4}$	$1.7 \times 10^{-5}$

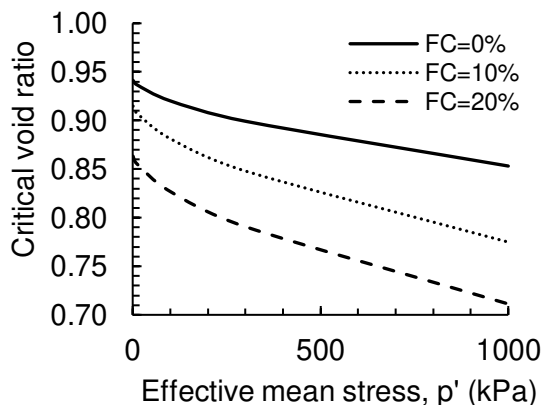


Figure 2. Variation of CSL with addition of fines in Toyoura sand

### 2.3.2 Calibrating SANISAND material parameters for offshore wind site soil

Having understood the effects of non-plastic fines on behaviour of sand and on SANISAND material parameters. Results of drained and undrained triaxial tests on reconstituted sand specimens (with fines content of 0 and 20 %) from an actual offshore wind farm site were used to calibrate the SANISAND material parameters for these two soils. The tests were carried out on samples consolidated at a mean effective stress of 126 kPa and with relative density of 80 %. It is to be noted that the experimental data was scarce for the accurate determination of all SANISAND material parameters. Figure 3 compare the predicted and experimental triaxial test results to evaluate the capacity of the calibrated material parameters to capture the behaviour of the two sands. It was concluded that the SANISAND model can successfully capture the main features of the material behaviour. The calibrated material parameters for two sands are tabulated in Table 2.

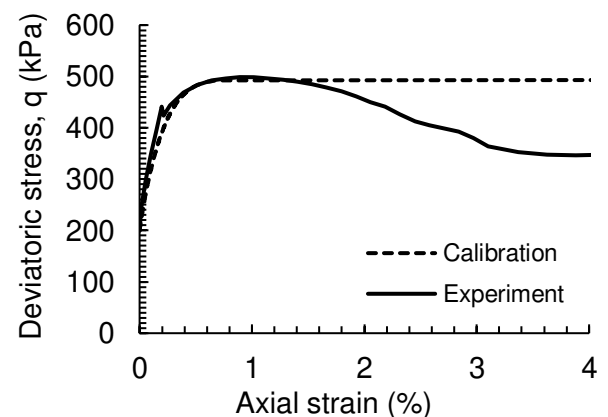
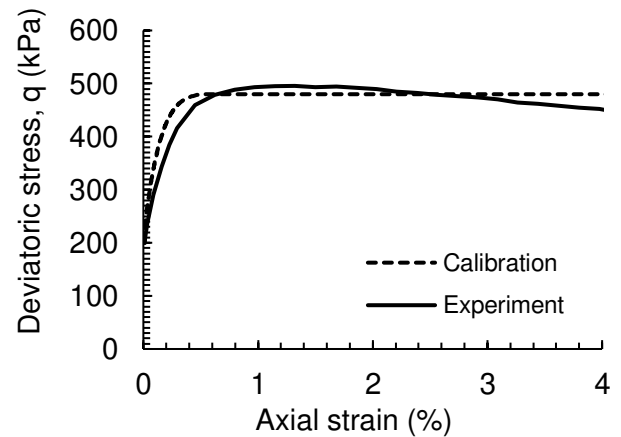


Figure 3. Predictions of drained triaxial stress-strain curve by calibrated material parameters for 0 % (above) and 20 % (below) FC

Table 2. SANISAND parameters for offshore wind farm site

Parameter	FC 0 %	FC 20 %
$G_0$ (-)	220	145
$\nu$ (-)	0.07	0.07
$M$ (-)	1.27	1.27
$c$ (-)	-	-
$\lambda_c$ (-)	0.008	0.0091
$e_0$ (-)	0.865	0.74
$\xi$ (-)	0.9	0.9
$m$ (-)	0.01	0.01
$h_0$ (-)	14	14
$c_h$ (-)	0.95	0.9
$n^b$ (-)	1.8	1.8
$A_0$ (-)	1	1
$n^d$ (-)	2	2
$z_{max}$ (-)	4	4
$c_z$ (-)	600	600

### 3 RESULTS AND DISCUSSIONS

This section discusses the effect of fines on CPTu tip resistance for the ideal case which involves Toyoura sand with varying fines content of 0, 10 and 20 %. Further, it includes comparisons of simulated CPTu data with actual CPTu measurements from an offshore wind farm site with both clean and silty sands (fines content of 2% and 17%).

#### 3.1 Influence of fines on tip resistance for Toyoura sand

Cone penetration tests were simulated at a penetration rate of 20 mm/s into the soil domain defined in section 2.1. An overburden stress of 100 kPa was considered for all simulation cases. The initial void ratio was set at 0.868 for all the cases. The soil was completely drained during the CPT penetration process implying that the soil was modelled to be dry (solid line in Figure 4). CPTu penetration was simulated until a constant tip resistance was observed. Figure 4 shows the simulated tip resistance development with time as the CPTu penetrates, for various fines content. It is evident that increasing fine content leads to a reduction in tip resistance. The effect of drainage and saturation is discussed in the upcoming sections.

#### 3.2 Influence of drainage on tip resistance for Toyoura sand

The soil drainage was considered under two circumstances: (1) soil was completely undrained during the CPT penetration process (dashed line in Figure 4), and (2) the soil was allowed to drain during the penetration process as excess pore pressures developed (dotted line in Figure 4). Drainage during penetration process was modelled as a coupled pore water flow and stress

equilibrium analysis available in ABAQUS standard. Figure 4 shows the tip resistance development with time as the CPTu penetrates soil for different drainage conditions. The tip resistance at undrained conditions is much lower even for sand without fines. This is due to development of positive excessive pore pressures during CPTu penetration which led to a reduction in effective stresses and lower tip resistance. Figure 5 shows the excess pore pressure contour around the tip of the CPT at the end of the penetration. Excess pore pressures generated right around the tip of the cone were also observed by Golestani and Ahmadi (2021). When the soil is allowed to drain while the CPTu penetrates, permeability of the soil plays a major role. It can be observed that sand without any fines led to nearly the same tip resistances as in the drained case. The permeability of soil drastically reduces (Table 1) with fines content eventually leading to much lower tip resistances as evident in Figure 4. Sand with 20 % fines demonstrated nearly undrained behaviour during CPTu penetration even if pore pressures were allowed to drain. Figure 6 describes the tip resistance values on the Roberson et al. (1986) diagram. The placement of tip resistance values on the diagram indicates that the material behaviour changes from that of a sand (0 %) to silty sand (10 %) to clay (20 %) with the addition of fines and reducing permeability.

#### 3.3 Simulation of CPTu in soil layers from offshore wind farm site

The results from the previous section demonstrated the capabilities of the framework to capture the effect of fines on tip resistance for different drainage conditions. But the primary motivation of the work is to be able to capture the effect of fines on tip resistances for offshore conditions. The CPTu measurements from two locations at an offshore wind farm site are of specific interest at a depth of 10 m and 19 m respectively as depicted in Figure 7. The soil layer at 10 m depth has a fines content of 2-3 % (Location 1) and that at 19 m depth a fines content of 17 % (Location 2) as depicted in Figure 8. Results from the triaxial tests on reconstituted sand from the same site were used to calibrate the SANISAND model, as described in section 2.3.2. It is to be noted that the calibrated material parameters for the sand with fines had a fines content of 20 % whereas the layer for which we have the CPT measurements has fines content of 17 %. The pore pressure measurements from the CPTu penetration results from the field indicated that there was no development of excess pore water pressures. Hence, all the simulations were carried out considering the soil layer to be completely drained and effective stress conditions at respective depths were assumed.

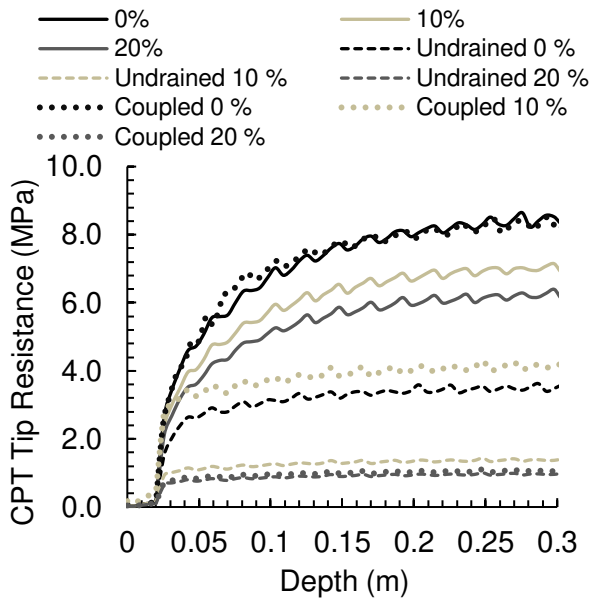


Figure 4. Variation of tip resistance for Toyoura sand with varying fines content and drainage conditions for 10 m overburden

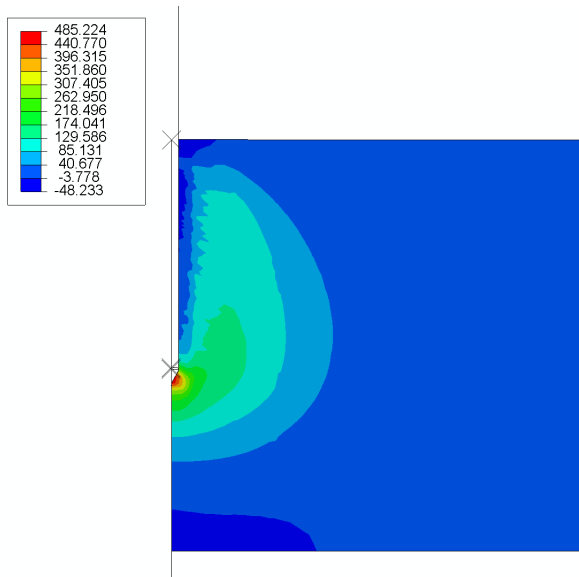


Figure 5. Excess pore water pressure contours around CPT at end of penetration for Toyoura sand with 0 % fines under undrained conditions

Two cases were simulated considering effective stress conditions at a depth of 10 m for sand layer without any fines and at 19 m depth for sand with 17 % of fines. The relative densities (with no correction for fines content) derived from the field data, as shown in Figure 7, were used to evaluate the initial void ratio for the numerical model. The material parameters were considered as per Table 2. Figure 8 depicts the tip resistance values from large deformation finite element method (LDFEM) simulations overlaid on the field CPTu values. For Location 1, it can be observed that the LDFEM simulation results exactly predict CPTu values at 10 m depth (essentially no fines content). For Location 2, the simulation results seem to underpredict the tip resistance

values at 19 m depth, and this could be since the material parameters used to simulate this soil layer are for 20 % fines whereas the soil layer on field has 17 % fines. As tip resistances values have been found to reduce with increasing fines content, this explains the under prediction of tip resistance values by the numerical framework. In addition, the initial void ratio was estimated considering  $Dr$  of 80 % for sand with 20 % fines whereas the relative density must be accordingly modified, as the sand under consideration has fines content of only 17 %. This scaling would reduce initial void ratio leading to more accurate predictions.

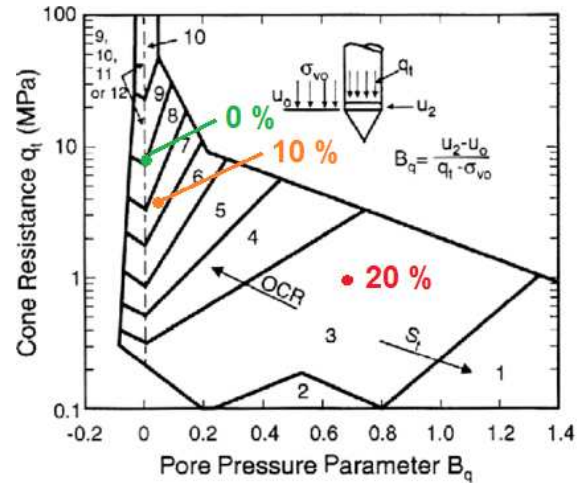


Figure 6. Tip resistance values under partially drained conditions on the Robertson diagram (Robertson et al., 1986)

#### 4 CONCLUSIONS

A finite element framework based on the Zipper technique was formulated to simulate CPTu involving large deformations. The SANISAND model was used to capture the soil behaviour of silty sands. Increasing fines content for a particular sand was simulated by varying the parameters governing the critical state line after Wei and Yang (2019). CPTu tip resistance was found to decrease with increasing fines content for Toyoura sand. Undrained conditions led to development of excess pore pressures, which further reduced tip resistance values. Further, CPTu simulations of tip resistance were conducted and compared to field measurements from two locations at an offshore wind farm site (with two different fines contents). Based on material parameters calibrated with triaxial tests on reconstituted specimens from the site, the numerical results were found to capture both qualitatively and quantitatively the influence of fines content on tip resistance. It is envisaged to use results from CPTu calibration chamber tests to verify the developed framework. The developed procedure can be extrapolated to establish a larger data set that can be used to develop a correlation that can help improve estimating the presence of fines from CPTu data based on relative density, vertical effective stress, and critical state parameters.



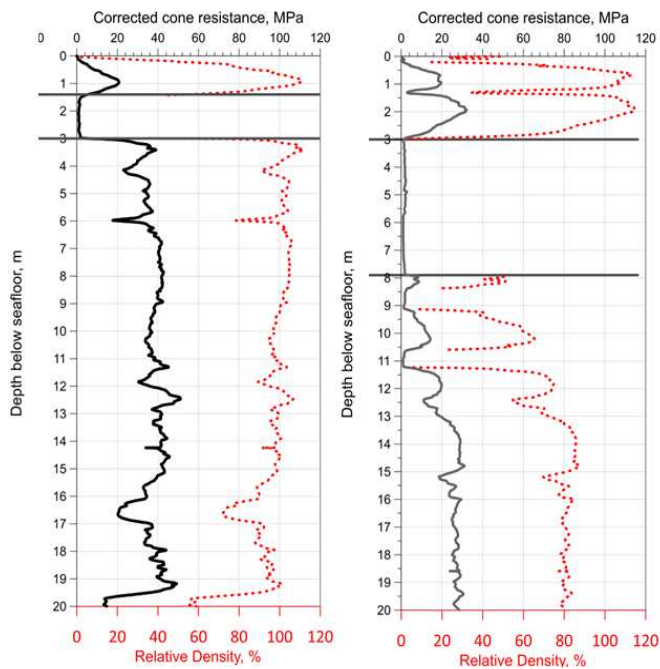


Figure 7 Cone tip resistance and relative density for two locations for an offshore wind farm site with 0 % fines (left) and 17 % fines (right)

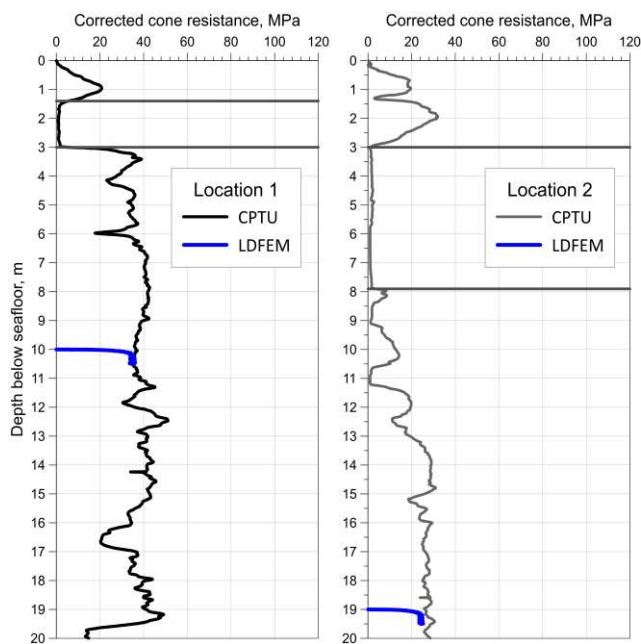


Figure 8. Comparison of numerically measured tip resistance values to field measurements in soil layers with 0 % fines (left) and 17 % fines (right)

## 5 ACKNOWLEDGEMENTS

This publication has been prepared as part of NorthWind (Norwegian Research Centre on Wind Energy) co-financed by the Research Council of Norway, industry and research partners, under project number 321954. Read more at [www.northwindresearch.no](http://www.northwindresearch.no).

## 6 REFERENCES

- Bassal, P.C., Boulanger, R.W., DeJong, J.T. 2022. Site-Specific CPT-Based Fines Content Correlations Using Percentile Matching. *Proceedings of Geo-Congress: Geophysical and Earthquake Engineering and Soil Dynamics*, 549-558
- Cetin, K.O., Ozan, C. 2009. CPT-Based Probabilistic Soil Characterization and Classification, *Journal of Geotechnical and Geoenvironmental Engineering* **135**(1).
- Chmelniczki, A., Nagula, S., Grabe, J. 2017. Numerical Simulation of Deep Vibration Compaction in Abaqus/CEL and MPM. *Procedia engineering* **175**, 302–309.
- Cudmani, R.O. 2001. *Statische, Alternierende Und Dynamische Penetration in Nichtbindigen Boden*, PhD Thesis, Institutes für Bodenmechanik und Felsmechanik der Universität Karlsruhe, Karlsruhe, Germany.
- Durgunoglu, H.T., Mitchell, J.K. 1975. Static penetration resistance of soils: II. Evaluation of theory and implications for practice. *Proceedings of the Conference on In Situ Measurement of Soil Properties ASCE*, 1, 172–189.
- Golestani Dariani, A.A., Ahmadi, M.M. 2021. Generation and Dissipation of Excess Pore Water Pressure During CPTU in Clayey Soils, *A Numerical Approach, Geotechnical and Geological Engineering* **39**, 3639–3653.
- Grabe, J., König, F. 2004. Zur Aushubbedingten Reduktion Des Drucksondierwiderstandes, *Bautechnik* **81**(7), 569–577.
- Idriss, I.M., Boulanger, R.W. 2008. *Soil Liquefaction During Earthquake*, EERI Publication, Monograph MNO-12, Earthquake Engineering Research Institute, Oakland, USA.
- Jostad, H.P., Dahl, B., Page, A., Sivasithamparam, N., Sturm, H. 2020. Evaluation of soil models for improved design of offshore wind turbine foundations in dense sand, *Géotechnique* **70**, 1-37. 10.1680/jgeot.19.TI.034.
- Kort, D.A., Pederstad, H.J., Nowacki, F. 2015. Planning of soil investigation for GBS foundation design. *Proceedings Frontiers in Offshore Geotechnics III*, 1073-1078.
- NREL 2022. Offshore wind market report, *US Department of Energy, Office of energy efficiency & renewable energy*, USA.
- Robertson, P.K. 1991. Soil classification using the cone penetration test: replay, *Canadian Geotechnical Journal* **38**(28), 176-178.
- Robertson, P.K., Wride, C.E. 1998. Evaluating cyclic liquefaction potential using the cone penetration test, *Canadian Geotechnical Journal* **35**, 442-459.
- Yang, S. 2004. Characterization of the properties of sand-silt mixtures, *Doctoral Thesis*, Norwegian University of Science and Technology, Trondheim, Norway.
- Yi, F. 2014. Estimating soil fines contents from CPT data. *Proceedings of 3<sup>rd</sup> International symposium on cone penetration testing*, Las Vegas, Nevada, USA.